ELSEVIER

Colloids and Surfaces A: Physicochem. Eng. Aspects 250 (2004) 409–414

COLLOIDS AND SURFACES A

www.elsevier.com/locate/colsurfa

The exponential power law: partial wetting kinetics and dynamic contact angles

Becky Lavi, Abraham Marmur*

Department of Chemical Engineering, Technion – Israel Institute of Technology, 32000 Haifa, Israel

Received 30 January 2004; accepted 27 April 2004
Available online 17 September 2004

Abstract

An equation for the kinetics of partial drop spreading is proposed. This equation was empirically derived from experimental data for the spreading kinetics of partially wetting liquids in terms of the wet area versus time. The equation has the form of an exponential power law (EPL), and transforms into the well-known power law for complete wetting, when the equilibrium contact angle approaches zero. The EPL fits very well available experimental data. To lend additional support to the validity of this generalized equation, it will be demonstrated that when it is transformed to present the dynamic contact angle (DCA), it fits very well DCA experimental data for other wetting processes, such as capillary flow and tape coating.

Keywords: Exponential power law; Wetting; Dynamic contact angle; Capillary flow; Contact angle; Spreading

1. Introduction

Wetting of solid surfaces by liquids is a central process in many practical applications [1–6]. Some examples include printing, painting, adhesion, lubrication and spraying on surfaces. Among the most common forms of wetting are spreading of a drop on a solid surface, penetration of liquids into capillary pores, and tape coating processes. Although wetting has been studied for many years, many fundamental problems are still open, especially those related to the motion kinetics of the contact line. A useful form of presentation of contact line kinetics is the time or velocity dependence of the dynamic contact angle (DCA), since the contact angle serves as a common denominator for studying the various wetting processes. The DCA has been correlated with the velocity of the contact line using a hydrodynamic approach [3,7–14], a molecular kinetics approach [15–18], a combined hydrodynamic-molecular kinetics approach [19–21], and an empirical approach [22–24].

Drop spreading is one of the most studied wetting processes from a fundamental point of view. In addition to DCA studies, the kinetics of drop spreading has been investigated by following the time dependence of the wet (solid–liquid) area. An important motivation for this approach has been the higher experimental accuracy in area measurements in comparison with contact angle measurements. In terms of the wet area, the kinetics of *complete* wetting (when the equilibrium contact angle is zero) can be well correlated by a power law [2–4,14,25–36]

$$A = K\tau^n \tag{1}$$

In this equation, A is the dimensionless drop base area, normalized with respect to $V^{2/3}$, where V is the drop volume, K and n are empirical coefficients, and τ is the dimensionless time, defined as

$$\tau \equiv \frac{\sigma}{\mu V^{1/3}} t \tag{2}$$

Here, σ is the surface tension of the liquid, μ, its viscosity, and t, the time. This dependence was developed on theoretical grounds [3,14,26–33], and empirically confirmed

* Corresponding author. Tel.: +972 4 829 3088; fax: +972 4 829 3088.
E-mail address: marmur@tx.technion.ac.il (A. Marmur).

0927-7757/$ – see front matter © 2004 Elsevier B.V. All rights reserved.
doi:10.1016/j.colsurfa.2004.04.079

[2,32,34–36]. The theoretically predicted values of the power, n, in Eq. (1) are within the range of 0.2–0.28. Experimentally obtained values of n are within the range of 0.2–0.29 with some exceptional values of 0.066 and 0.627 [2].

Regarding the kinetics of *partial* wetting of drops (when the equilibrium contact angle is higher than zero), no generalization of Eq. (1) to partial wetting has yet been reported [8,13,28,35–39]. In addition, there is a need for more experimental data for the kinetics of partial wetting of drops. Therefore, the objectives of this paper are: (a) to present additional experimental data for partial wetting kinetics of drops, in terms of the time dependence of the wet area, and (b) to present a generalization of the power law, Eq. (1), for the partial wetting regime, and show its agreement with the experimental data. To lend additional support to the validity of this generalized equation, it will be demonstrated that when it is transformed to present the DCA, it fits very well DCA experimental data for other wetting processes, such as capillary flow and tape coating.

2. Experimental

Fig. 1 shows the experimental system. The system was very simple and consisted of a horizontal plate (1) onto which the tested solid surface (2) was placed. The liquid drop was placed on the solid surface using a syringe with a bent needle (3). The process of spreading of the drop on the solid surface was recorded using a high-speed video camera (Redlake, model 2000 s), (4). The process was recorded as a sequence of frames (500 frames/s) using a frame grabber (Media Cybernetics, Pro-Series Capture Kit). Out of all the grabbed frames for each experiment, about 100 were selected and analyzed with an image analysis software (Media Cybernetics, Image Pro Plus 4) to find out the drop base area as a function of time. The time reading was taken and recorded by the camera. The room temperature was kept at $24 \pm 2\,^{\circ}C$, and the relative humidity at $46 \pm 5\%$. Every experiment was repeated at least three times, and the data presented below are the averages of the repeated results. Data were considered acceptable only if for three repetitions, the data for each time point differed by less than 10%.

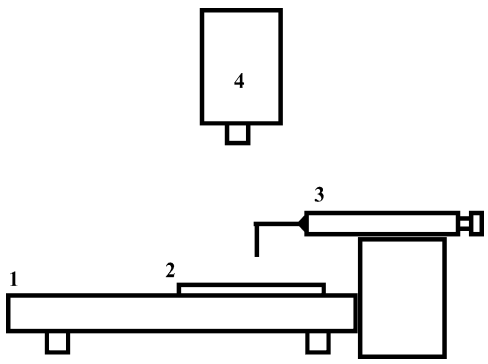

Fig. 1. The experimental system.

Table 1
Physical properties of the liquids used for the drop spreading experiments

Liquid	Density (kg/m^3)	Viscosity (Pa s)	Surface tension (mN/m)
Squalane (Aldrich, 99%)	809	34.0×10^{-3}	32.0
Hexadecane (Fluka, 99%)	773	3.07×10^{-3}	27.0
Tetradecane (Fluka, 98%)	749	2.04×10^{-3}	25.3
Cycloheptanol (Fluka, 97%)	948	23.4×10^{-3}	32.8
Cyclooctanol (Fluka, 98%)	974	62.2×10^{-3}	40.9

The solid surface was a hydrophobic, homogeneous, monolayer-coated silicon wafer. The monolayer was prepared with Dodecyltrichlorosilane (DTS) as follows:

1. Rinsing the wafers in continuously renewed condensed chloroform (Bio Lab, 99.9%) for 15 min.
2. UV irradiating of the wafers under oxidizing ozone surroundings for 15 min.
3. Immersing the wafer in a solution that consists of 18 ml Bicyclohexyl (Fluka, 99%) and 18 μl Dodecyltrichlorosilane (Aldrich, 98%) for 1 h.
4. Rinsing in continuously renewed condensed chloroform for 15 min.
5. Immersing in the Bicyclohexyl solution for 15 min.
6. Repeating steps 4 and 5 three times.

The coated silicone wafers were cleaned before the experiments by rinsing in continuously renewed condensed chloroform for 15 min.

The liquids used for the spreading studies and their physical properties are listed in Table 1. All the liquids partially wet the coated silicon wafer. The drop volume was measured by weighing the drop immediately after the spreading process was finished. Comparison of the time needed for a meaningful evaporation of the drop with the time of the experiment revealed that there was no significant evaporation during the experiment. Therefore, the drop volume was considered constant throughout the spreading process.

3. Results and discussion

Experimental data for the kinetics of partial drop spreading are presented in Fig. 2. The data are presented in terms of the relative dimensionless wet area, A/A_f, versus τ, where A_f is the final, equilibrium value of the normalized wet (solid–liquid) area. In addition to our experimental data, Fig. 2 includes two sets of data from the literature [40,41] that measured and reported the kinetics of partial drop spreading in terms of the wet area.

Based on the qualitative behavior of the experimental data in Fig. 2, the following equation for the kinetics of partial drop spreading is suggested

$$\frac{A}{A_f} = 1 - \exp\left(-\frac{K}{A_f}\tau^n\right) \tag{3}$$

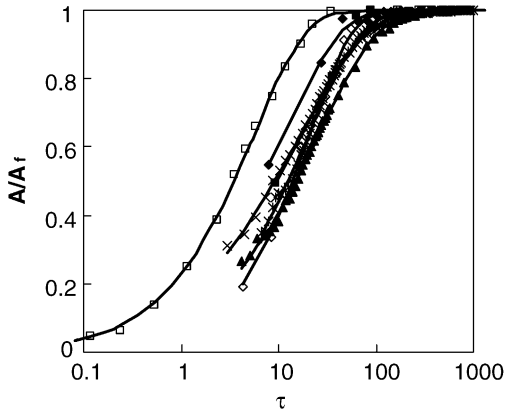

Fig. 2. Drop spreading kinetics of various liquids – relative dimensionless wet area vs. dimensionless time. (■) Tetradecane, (♦) Hexadecane, (▲) Squalane, (×) Cycloheptanol, and (*) Cyclooctanol on a DTS coated silicone wafer, (□) Polyisobutylene on Polytetraflouroethylene [40], and (◊) Ethylene glycol on hydrophobic glass [41]. The solid curves represent the best fits of Eq. (3) to the experimental data.

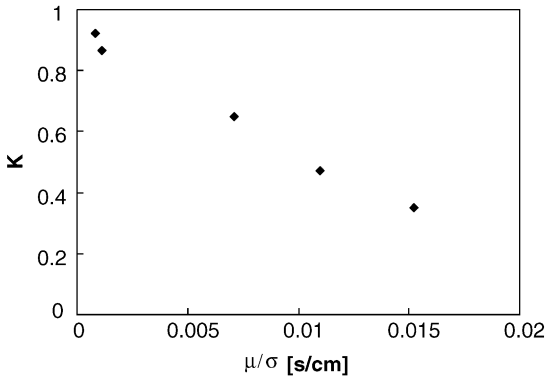

Fig. 3. The dependence of the parameter K in Eq. (3) on the ratio μ/σ.

This equation will be referred to below as the "exponential power law" (EPL). It is important to notice that Eq. (3) transforms into Eq. (1) for complete wetting. This is so, since for complete wetting $A_f \to \infty$; therefore, $\exp(-K\tau^n/A_f) \approx 1-K\tau^n/A_f$. Consequently,

$$A \to K\tau^n$$

Eq. (3) defines time zero at drop impact, when the wet area is zero, but this time is not always accessible from an experimental point of view. Therefore, an additional empirical parameter, τ_o, was added, such that $\tau \equiv \tau_{exp} + \tau_\circ$, where τ_{exp} is the dimensionless time recorded by the camera from the first frame at which the drop touches the solid surface. Thus, in order to fit Eq. (3) to experimental data, the values of K, n, A_f, and τ_o have to be determined, under the constraint that they all must be non-negative. The best fits of Eq. (3) to the sets of experimental data in Fig. 2 are presented by the curves in this figure. It can be seen that the agreement between the EPL, Eq. (3), and the experimental data is excellent. Values of K, n, A_f, and τ_o are shown in Table 2, along with the correlation coefficients, R^2. As shown in this table, the value of R^2 for each line in Fig. 2 is larger than 0.999. The values of n for partial wetting are found to be higher than for complete wetting. In general, Table 2 shows a rough trend of n increasing with θ_e, however, more data are required to establish such a correlation. The parameter K is found to decrease linearly with the ratioμ/σ as shown by Fig. 3. This dependence of K is reasonable, since it indicates that the kinetics is quicker as the viscosity is lower and the surface tension is higher.

As mentioned in Section 1, the common denominator for all wetting processes is the DCA, which is usually correlated with the capillary number, $Ca \equiv \mu v/\sigma$, where v is the velocity of the contact line. Therefore, it is useful to transform the EPL, Eq. (3), into an expression for the dependence of the DCA on Ca. The dimensionless wet area of the drop can be easily expressed in terms of the contact angle, θ, by assuming that the drop shape is a spherical cap

$$A = \pi \sin^2\theta \left[\frac{3}{\pi(1-\cos\theta)^2(2+\cos\theta)}\right]^{2/3} \quad (4)$$

The capillary number is derived from Eq. (3) by differentiating it to get the velocity of the contact line, $v = dr/dt$, where r is the radius of the wet area

$$Ca = \frac{1}{2}\frac{Kn}{\sqrt{\pi A_f}}\tau^{n-1}\exp\left(\frac{-K}{A_f}\tau^n\right)\left[1-\exp\left(\frac{-K}{A_f}\tau^n\right)\right]^{-1/2} \quad (5)$$

In order to present the DCA versus Ca, the DCA is calculated from Eqs. (3) and (4), while Ca is calculated from Eq. (5), for the same value of τ. The abbreviation EPL-DCA will be assigned to this form of presentation. Fig. 4 (thick full curves)

Table 2
Parameters calculated by the best fits of Eq. (3) to drop spreading experimental data

Liquid	Solid	K	n	τ_o	$A_f/V^{2/3}$	θ_e (degrees)	R^2
Tetradecane	DTS[a]	0.924	0.647	9.31	5.75	30.5	0.9997
Hexadecane	DTS[a]	0.866	0.736	8.03	5.07	35.9	1
Squalane	DTS[a]	0.471	0.699	4.13	4.49	41.5	0.9999
Cycloheptanol	DTS[a]	0.648	0.618	2.96	3.67	53.5	0.9999
Cyclooctanol	DTS[a]	0.352	0.775	6.62	3.60	54.2	0.9999
PIB[b] [40]	PTFE[c]	0.884	0.797	0	3.44	59.6	0.9998
Ethylene glycol [41]	Hydrophobic glass	0.166	0.964	0	3.05	61.5	0.9996

[a] DTS – Dodecyltrichlorosilane-coated silicon wafer.
[b] PIB – Polyisobutylene.
[c] PTFE – Polytetraflouroethylene.

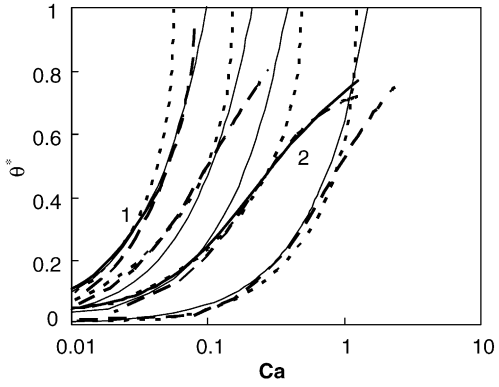

Fig. 4. Drop spreading kinetics of various liquids — dimensionless dynamic contact angle vs. capillary number. The thick solid curves represent the best fits of the EPL-DCA correlation (Eqs. (3)–(5)) to experimental data for: (1) Ethylene glycol on hydrophobic glass [41], (2) Polyisobutylene on Polytetraflouroethylene [40]. Dashed curves — Eq. (7) for a range of values of B (0.3–1) and C (0.006–0.16). Thin solid curves — Eq. (8) for a range of values of D (2–34). Thick dashed curves — Eq. (9) for a range of values of ρ^s_{1e} (0.35–0.6), ρ^s_{2e} (0.19–0.63) and Yu (1.4–9).

shows the EPL, Eq. (3), translated into the DCA versus Ca form. These curves were calculated for the data of Zosel [40] and Von Bahr et al. [41], because they cover the largest range of Ca. For clarity of the figure, only the theoretical curves are shown and not the raw experimental data (their excellent agreement was demonstrated in Fig. 2). The DCA is presented as a dimensionless variable

$$\theta^* \equiv \frac{\theta_d^3 - \theta_e^3}{\pi^3 - \theta_e^3} \tag{6}$$

where θ_d is the DCA and θ_e, the equilibrium contact angle. This form of normalization was chosen in order to limit the range of θ^* to be from zero to one. The dependence on θ^3 was chosen on the basis of previous theoretical correlations [3,8,9]. The values of θ_e were calculated from the A_f values, using Eq. (4). Table 2 also shows the values of θ_e for all the drop spreading systems.

To compare the EPL-DCA curves with previous correlations for the DCA, three frequently cited correlations, the Blake and Haynes model [15], the Cox equation [9], and the Shikhmurzaev equation [11,46] were used. These three correlations have theoretical backgrounds: the Blake and Haynes model [15] is based on a molecular kinetics description of the movement of the contact line

$$\cos\theta_d = \cos\theta_e - B\sinh^{-1}\left(\frac{Ca}{C}\right) \tag{7}$$

where $B \equiv n'kT/\sigma$ and $C \equiv 2f\lambda\mu/\sigma$. Here, n' is the number of adsorption sites per unit area of the solid surface, k, the Boltzmann constant, T, the absolute temperature, f, the frequency of molecular displacements in a static contact line, and λ, the average distance between adsorption sites.The equation of Cox [9], which was obtained from a hydrodynamic treatment of the contact line motion, is

$$\theta_d^3 = \theta_e^3 + 9DCa \tag{8}$$

where $D \equiv \ln(L/s)$, L is the characteristic length of the system and s, the slip length. The Shikhmurzaev equation is also based on hydrodynamic principles, but, in addition, takes into account the formation and disappearance of interfaces during the movement of the contact line and the existence of surface tension gradients in the neighborhood of the moving contact line.

$$\cos\theta_d = \cos\theta_e - \frac{2\left|\rho^s_{2e} + \rho^s_{1e}u_o(\theta_d)\right|}{(1-\rho^s_{1e})[(1+\rho^s_{2e}/V^2)^{1/2}+1]} \tag{9}$$

where ρ^s_{1e} and ρ^s_{2e} are the equilibrium surface density of the liquid–gas interface and the solid–liquid interface, respectively, $u_o(\theta_d)$ is the tangential component of the free surface velocity in a reference frame moving with the contact line. If the influence of other boundaries on the flow in the vicinity of the contact line can be neglected and the free surface is approximately planar, then

$$u_o(\theta_d) = \frac{\sin\theta_d - \theta_d\cos\theta_d}{\sin\theta_d\cos\theta_d - \theta_d} \tag{10}$$

V is the dimensionless contact line speed, which is related to Ca by

$$V = Yu\cdot Ca \quad , Yu = \left[\frac{\sigma\tau\beta}{\mu\rho^s_o\gamma(1-4\alpha\beta)}\right]^{1/2} \tag{11}$$

where τ is the relaxation time of the surface properties, ρ^s_o, the solid–liquid surface density corresponding to zero surface pressure, γ, a phenomenological coefficient of that interface and α and β are constants which characterize viscous properties of the interface.

Fig. 4 also shows Eq. (7) (dashed curves), Eq. (8) (thin full curves), and Eq. (9) (dashed bold curve) for a range of values of their parameters (B, C, D, ρ^s_{1e}, ρ^s_{2e} and Yu). It is clearly demonstrated that the Shikhmurzaev equation may fit the experimental data for a wide range of capillary numbers, as do the EPL-DCA curves. The Blake and Hynes equation and Cox equation may agree with the experimental data only for low capillary numbers. At higher capillary numbers, the curves representing the experimental data have an inflection point, which is neither predicted by Eq. (7) nor by Eq. (8), but is predicted by the EPL-DCA correlation and by Eq. (9). It should be remembered, however, that the theories of Blake and Hynes [15] and of Cox [9] were developed to begin with only for low capillary numbers.

To show that the EPL is useful for wetting processes in general, experimental data for other wetting systems should be compared with the EPL-DCA correlation. First, comparison is made with DCA data for flow in capillaries [42,43], as shown in Fig. 5a. The thick full curves represent the best fit of the EPL-DCA correlation, Eqs. (3)–(5), to the experimental data. Table 3 presents the parameters that yielded the best fits and the corresponding correlation coefficients. As can be

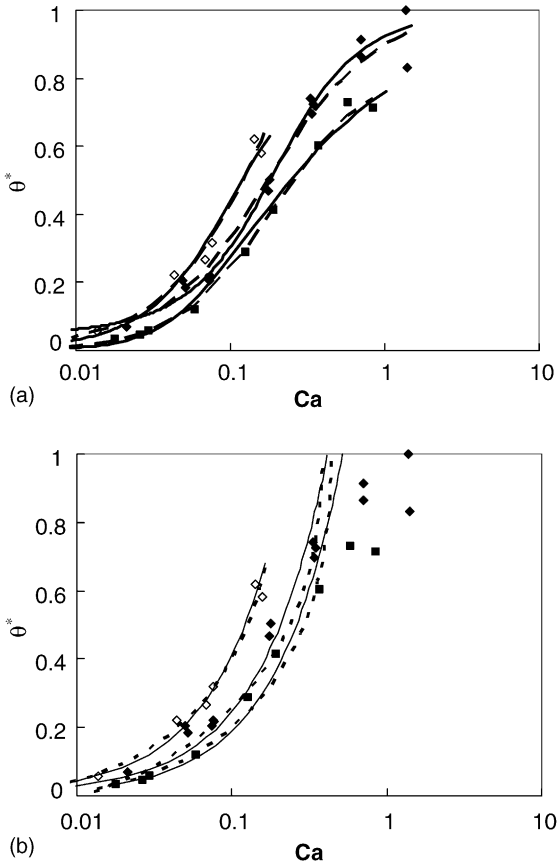

Fig. 5. Dimensionless dynamic contact angle vs. capillary number for flow in glass capillaries. (◊) Santicizer 405 [32], (♦) Admex 760 [32], (■) Silicone oil [31]. (a) Thick solid curves and thick dashed curve – best fits of the EPL-DCA correlation (Eqs. (3)–(5)) and Eq. (9), respectively, to the experimental data; (b) dashed curves and thin, solid curves – best fits of Eqs. (7) and (8), respectively, to the experimental data by the procedure described in the text.

seen in Fig. 5a and Table 3, the EPL-DCA correlation fits very well to the experimental data. The experimental data can be also compared with the above-mentioned previous correlations, Eqs. (7)–(9). Fig. 5a also shows the good agreement between the experimental data and Eq. (9), which gave values of R^2 roughly equal to those obtain by the EPL-DCA fitting. Fig. 5b shows the comparison of Eqs. (7) and (8) to the experimental data. The qualitative behavior of the experimental data at relatively high *Ca* is different than that predicted by these equations; therefore, the fitting of Eqs. (7) and (8) to the experimental data was done by successively removing experimental points for the higher *Ca*, until the correlation coefficient became roughly equal to the value achieved by the EPL-DCA approach. Indeed, Fig. 5b demonstrates that the correspondence is very good only for relatively low *Ca*.

Table 3
Parameters calculated by the best fits of the EPL-DCA correlation to capillary flow experimental data

Data source	Liquid	Solid	EPL-DCA			
			K	n	θ_e (degrees)	R^2
Hoffman [32]	Santicizer 405	Glass	0.304	1.02	65.6	0.987
Hoffman [32]	Admex 760	Glass	0.430	1.13	84.2	0.987
Fermigier & Jenffer [31]	Silicone oil	Pyrex	0.719	0.751	26.0	0.991

Fig. 6a and b show various sets of experimental data for tape wetting, either by bath drawing [17,44,45] or by a liquid curtain [46]. The fitting of the EPL-DCA correlation and Eqs. (7)–(9) to the experimental data was done in the same way as for the capillary flow data. The parameters that yielded the best fits of the EPL-DCA to the experimental data are shown in Table 4. The curves for the EPL-DCA correlation and for Eq. (9) are shown in Fig. 6a. For the sake of clarity, the correlations are presented only for four sets of data. It can be concluded from this figure and from Table 4 that the EPL-DCA correlation fits very well also to the tape wetting data, as does Eq. (9). The predictions of Eqs. (7) and (8) are shown in Fig. 6b. As before, they fit very well to the data for

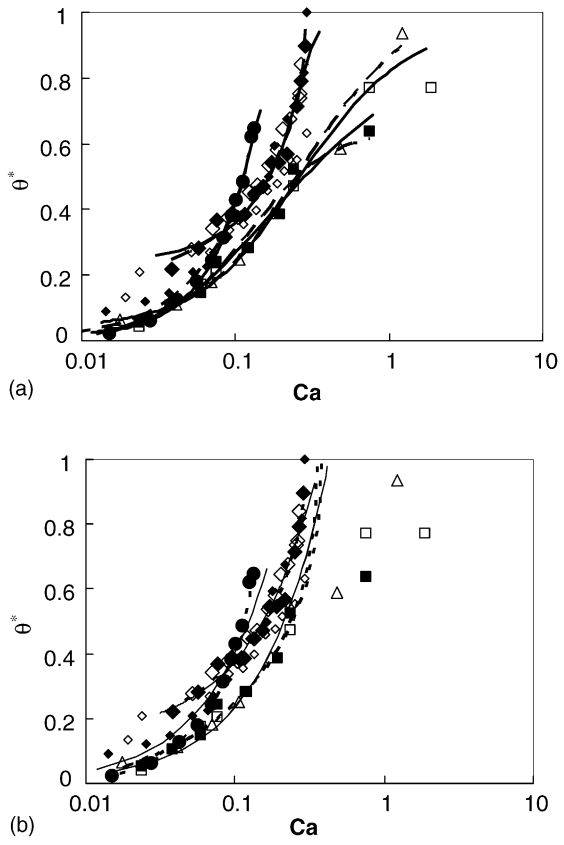

Fig. 6. Dimensionless dynamic contact angle vs. capillary number for tape wetting. (●) Water on Polyethyleneterephtalate (PET) tape [17], (◊) aqueous glycerol curtain on PET at $Q = 3.76\,cm^2/s$ [46], (♦) aqueous glycerol curtain on PET at $Q = 3.22\,cm^2/s$ [46], (◊) aqueous glycerol curtain on PET at $Q = 1.88\,cm^2/s$ [46], (♦) aqueous glycerol on PET tape [46], (▲) castor oil on gelatin-coated Polystyrene tape [44], (□) Silicone oil III on Polytetraflouroethylene tape [45], (■) Silicone oil III on PS tape [45]. (a) Thick solid curves and thick dashed curve – best fits of the EPL-DCA correlation (Eqs. (3)–(5)) and Eq. (9), respectively, to the experimental data; (b) dashed curves and thin, solid curves – best fits of Eqs. (7) and (8), respectively, to the experimental data by the procedure described in the text.

Table 4
Parameters calculated by the best fits of the EPL-DCA correlation to tape wetting experimental data

Data source	Liquid	Solid	Wetting system	EPL-DCA			
				K	n	θ_e (degrees)	R^2
Blake [17]	Water	PET[a]	Tape	0.112	1.59	88.1	0.998
Blake et al. [46]	Aqueous glycerol	PET[a]	Tape	0.255	1.33	85.7	0.983
Blake et al. [46]	Aqueous glycerol	PET[a]	Curtain $Q = 3.76\,cm^2/s$	0.273	1.53	115	0.986
Blake et al. [46]	Aqueous glycerol	PET[a]	Curtain $Q = 3.22\,cm^2/s$	0.262	1.70	116	0.960
Blake et al. [46]	Aqueous glycerol	PET[a]	Curtain $Q = 1.88\,cm^2/s$	0.573	1.00	98.9	0.978
Gutoff et al. [44]	Castor oil	Gelatin coated PS[b]	Tape	0.723	0.976	79.9	0.984
Strom et al. [45]	Silicone oil III	PS[b]	Tape	0.822	0.709	34.5	0.990
Strom et al. [45]	Silicone oil III	PTFE[c]	Tape	0.659	0.810	29.9	0.991

[a] PET – Polyethyleneterephtalate.
[b] PS – Polystyrene.
[c] PTFE – Polytetraflouroethylene.

relatively low *Ca*, but cannot predict the inflection point that is typical of the behavior at higher *Ca*.

In summary, the empirically derived exponential power law predicts very well the kinetics of partial drop spreading. Moreover, the transformation of the EPL into a DCA versus *Ca* correlation (EPL-DCA) fits very well DCA experimental data for other wetting systems, such as capillary flow and tape wetting. Most importantly, the EPL-DCA correlation is successful at high as well as low capillary numbers. The EPL, and consequently its EPL-DCA derivative, is admittedly empirical. It is hoped, however, that its remarkable success in correlating experimental data for various wetting systems will trigger work on its theoretical justification.

References

[1] E.B. DussanV, Ann. Rev. Fluid Mech. 11 (1979) 371.
[2] A. Marmur, Adv. Colloids Interface Sci. 19 (1983) 75.
[3] P.G. de Gennes, Rev. Modern Phys. 57 (3) (1985) 827.
[4] A.M. Cazabat, Contemporary Phys. 28 (4) (1987) 347.
[5] L. Leger, J.F. Joanny, Rep. Prog. Phys. 55 (4) (1992) 431.
[6] J. De Coninck, M. de Ruijter, M. Voue, Curr. Opin. Colloid Interface Sci. 6 (2001) 49.
[7] C. Huh, L.E. Scriven, J. Colloid Interface Sci. 35 (1) (1971) 85.
[8] O.V. Voinov, Fluid Dynamics 11 (1976) 714.
[9] R.G. Cox, J. Fluid Mech. 168 (1986) 169.
[10] E. Ruckenstein, Langmuir 8 (1992) 3038.
[11] Y.D. Shikhmurzaev, J. Fluid Mech. 334 (1997) 211.
[12] K. Ishimi, J. Mohri, H. Mukouyama, H. Ishikawa, J. Chem. Eng. Jpn. 31 (6) (1998) 914.
[13] A.B.A. Elyousfi, A.K. Chesters, A.M. Cazabat, S. Villette, J. Colloid Interface Sci. 207 (1998) 30.
[14] S.N. Reznik, A.L. Yarin, Phys. Fluids 14 (1) (2002) 118.
[15] T.D. Blake, J.M. Haynes, J. Colloid Interface Sci. 30 (3) (1969) 421.
[16] R.L. Hoffman, J. Colloid Interface Sci. 94 (2) (1983) 470.
[17] T.D. Blake, Wettability, in: J.C. Berg (Ed.), Surfactant Science Series, vol. 49, Marcel Dekker, New York, 1993, p. 251.
[18] B.W. Cherry, C.M. Holmes, J. Colloid Interface Sci. 29 (1) (1969) 174.
[19] P.G. Petrov, J.G. Petrov, Langmuir 8 (7) (1992) 1762.
[20] M.J. de Ruijter, J. De Coninck, G. Oshanin, Langmuir 15 (1999) 2209.
[21] J.G. Petrov, J. Ralston, M. Schneemilch, R.A. Hynes, J. Phys. Chem. B 107 (2003) 1634.
[22] M. Bracke, F. De Voeght, P. Joos, Prog. Colloid Polym. Sci. 79 (1989) 142.
[23] P. Van Remoortere, P. Joos, J. Colloid Interface Sci. 160 (1993) 387.
[24] T.S. Jiang, S.G. Oh, J.C. Slattery, J. Colloid Interface Sci. 69 (1) (1979) 74.
[25] J. Lopez, C.A. Miller, E. Ruckenstein, J. Colloid Interface Sci. 56 (1976) 460.
[26] L.H. Tanner, J. Phys. D 12 (1979) 1473.
[27] G.F. Teletzke, H.T.L. Davis, E. Scriven, Chem. Eng. Commun. 55 (1-6) (1987) 41.
[28] P. Ehrhard, S.H. Davis, J. Fluid Mech. 229 (1991) 365.
[29] A.E. Seaver, J.C. Berg, J. Appl. Polym. Sci. 52 (1994) 431.
[30] C.-M. Lin, R.M. Ybarra, P. Neogi, Adv. Colloid Interface Sci. 67 (1996) 185.
[31] Y. Gu, D. Li, Colloids Surf., A 142 (1998) 243.
[32] F. Rieutord, O. Rayssac, H. Moriceau, Phys. Rev. E 62 (5) (2000) 6861.
[33] O.V. Voinov, J. Colloid Interface Sci. 226 (2000) 22.
[34] E.C. Chen, J.C.K. Overall, C.R. Phillips, Can. J. Chem. Eng. 52 (1974) 71.
[35] P. Levinson, A.M. Cazabat, M.A. Cohen-Stuart, F. Heslot, S. Nicolet, Revue de Physique Appliquee 23 (1988) 1009.
[36] P. Ehrhard, J. Fluid Mech. 257 (1993) 463.
[37] L.M. Hocking, A.D. Rivers, J. Fluid Mech. 121 (1982) 425.
[38] Y.D. Shikhmurzaev, Phys. Fluids 9 (2) (1997) 266.
[39] J. Fukai, M. Tanaka, O. Miyatake, J. Chem. Eng. Jpn. 31 (3) (1998) 456.
[40] A. Zosel, Colloid Polym. Sci. 271 (1993) 680.
[41] M. Von Bahr, F. Tiberg, V. Yaminsky, Colloids Surf. A: Physicochem. Eng. Aspects 193 (2001) 85.
[42] R.L. Hoffman, J. Colloid Interface Sci. 50 (2) (1975) 228.
[43] M. Fermigier, P. Jenffer, J. Colloid Interface Sci. 146 (1) (1991) 226.
[44] E.B. Gutoff, C.E. Kendrick, AIChE J. 28 (3) (1982) 459.
[45] G. Strom, M. Fredriksson, P. Stenius, B. Radoev, J. Colloid Interface Sci. 134 (1) (1992) 107.
[46] T.D. Blake, M. Bracke, Y.D. Shikhmurzaev, Phys. Fluids 11 (8) (1999) 1995.